Journal of Catalysis 281 (2011) 362–370

Contents lists available at ScienceDirect

Journal of Catalysis

journal homepage: www.elsevier.com/locate/jcat

# New efficient and long-life catalyst for gas-phase glycerol dehydration to acrolein

P. Lauriol-Garbey [a], J.M.M. Millet [a,*], S. Loridant [a], V. Bellière-Baca [b], P. Rey [c]

[a] Institut de Recherches sur la Catalyse et l'Environnement de Lyon, IRCELYON, UMR5256 CNRS-Université Claude Bernard Lyon 1, 2 avenue A. Einstein, F-69626 Villeurbanne cedex, France
[b] Rhodia, 52 rue de la Haie Coq, 93308 Aubervilliers cedex, France
[c] Adisseo, Antony Parc 2, 10 Place du Général de Gaulle, 92160 Antony, France

ARTICLE INFO

*Article history:*
Available online 23 June 2011

*Keywords:*
Niobium oxide supported on zirconia
Heterogeneous acid catalysis
Interaction with support
Stability on stream
Dehydration
Glycerol
Acrolein

ABSTRACT

Zirconium and niobium mixed oxides have been shown to be selective catalysts for dehydration of glycerol to acrolein, at 300 °C in the presence of water. The catalysts exhibit a selectivity to acrolein of approximately 72%, at nearly total glycerol conversion. More selective catalysts have been designed for this reaction, but whereas all of these are almost completely deactivated after only 24 h, ZrNbO catalysts still exhibit 82% conversion efficiency after 177 h on stream, its acrolein selectivity remaining unimpaired. Catalysts have been characterized by various techniques, showing that active and selective sites are weak or moderately acid Brønsted sites, whose presence is related to that of polymeric niobium oxide species in interaction with the zirconia support. The key stability of the catalysts has been attributed to the neutralization of Lewis acid of uncovered zirconia, which are unselective coke initiator sites.



## 1. Introduction

With the irrevocable decrease in the availability of raw fossil materials, a changeover of the chemical industry to renewable feedstock is needed. Because it will be produced in large quantities, as a co-product with biodiesel, glycerol is a potential initial building block for the production of many chemicals. Numerous studies have thus been undertaken to develop means to exploit glycerol in the most valuable manner. Among the more intensively studied examples of such developments, is the dehydration of glycerol to yield acrolein, which is an important intermediate chemical for the agro-industry [1–3].

Although a liquid-phase medium, including sub and supercritical water, has been proposed to run the reaction, the gas-phase remains the most economically viable method, even though a diluted aqueous solution of glycerol has to be used as starting material, and vaporized above 250 °C [2,3]. Several acidic catalysts have been proposed in recent years, for the gas-phase selective conversion of glycerol into acrolein [4–20]. Three types of catalyst allow the reaction to run successfully: (i) zeolites [4–9], (ii) heteropolyacids supported or unsupported [10–14], and (iii) supported oxides [15–18]. All of these exhibit high catalytic properties, at temperatures in the range between 260 °C and 350 °C, with an acrolein selectivity ranging between 70% and 80% at total glycerol conversion. Although most of the studies appear to agree on the fact that Brønsted acid sites are more efficient than Lewis acid sites, they lead to contradictory results concerning the nature and strength of the catalytic acid sites, which are efficient for the reaction. One study reported that the catalyst's efficiency in acrolein synthesis was enhanced by medium acidity ($-8.2 < H_0 < 3.0$) [21], whereas another study concluded that weak acidity was more appropriate [20], and yet another reported that the best selectivity to acrolein was obtained with strong acidic catalysts [14]. Given these discrepancies, it is likely that other parameters, such as the number and distribution of acid sites at the surface of the catalysts, may be the key to the catalyst's properties. Tolerance to water has also been proposed as a key parameter in the case of heteropolyacids [14].

Although most catalytic systems lead to a high selectivity to acrolein at total glycerol conversion, very few maintain their catalytic properties for more than 5–10 h. Although the catalyst deactivation is due to extensive coke deposition on its surface, attempts to limit the rate of coking by adding $O_2$ or $H_2$ in the gas phase, and modifying (or not) the catalysts, have not been convincingly successful [14,22]. Catalyst regeneration by means of coke combustion has also been periodically attempted *ex situ*, but until present this has again met with only limited success.

In the present study, we report on the development of new catalysts, which are both efficient for the dehydration of glycerol into acrolein, and more stable than those already proposed [4–20]. These catalysts, which correspond to NbZrO mixed oxides, are described in this paper. The most efficient NbZrO mixed oxide catalysts appear to be complex, with several phases. A comparative study of various pure or supported phases was thus needed in order to identify and characterize the active phase of such catalysts. The effects of different catalytic reaction parameters or catalyst characteristics have been studied, to optimize the process and

DOI of original articles: 10.1016/j.jcat.2011.05.013, 10.1016/j.jcat.2011.03.005
* Corresponding author. Fax: +33 4 72 44 53 99.
*E-mail address:* Jean-marc.millet@ircelyon.univ-lyon1.fr (J.M.M. Millet).

0021-9517/$ - see front matter © 2011 Elsevier Inc. All rights reserved.
doi:10.1016/j.jcat.2011.05.014

demonstrate possible regeneration of the catalyst. Finally, the characterization of the acid–base properties of these catalysts has been undertaken, in an effort to determine which of the catalysts' sites were active, selective, or unselective.

## 2. Experimental

### 2.1. Preparation of catalysts

#### 2.1.1. Preparation of ZrNbO catalysts

The preparation method is based on the work of Kantcheva et al. [23], consisting in impregnating hydrated zirconium oxide with a peroxo-niobate solution. However, in order to avoid the use of peroxo-niobate leading to a strongly exothermic reaction difficult to control, the impregnation was conducted in acidified water with ammonium oxalato-niobate. Twenty-four mmol of ammonium oxalato-niobate $Nb(NH_4)(C_2O_4)_2NbO{\cdot}xH_2O$ (Aldrich, 99.99%) were first dissolved into 65 mL of de-ionized water acidified at pH < 0,5 with concentrated nitric acid. The solution was then heated about 40 min at 45 °C in order to dissolve the niobium compound and cooled at room temperature before the addition of hydrated zirconia. The reaction medium was maintained for 24 h at 25 °C under stirring, and the solid was separated by filtration. The solid obtained were calcined under air at 600 °C for 2 h (heating rate 5 °C $min^{-1}$). The heating protocol involved two steps at 350 and 450 °C to eliminate the remaining nitrates. The samples obtained were denoted as ZrNbO-*x*, with *x* the Zr/Nb ratio.

#### 2.1.2. Preparation of bulk and supported pure phases

Tetragonal zirconia (*t*-$ZrO_2$) has been prepared by calcination of a zirconium hydroxide also synthesized by co-precipitation at pH 8.8 from a 0.4 M solution of zirconyl nitrate ($ZrO(NO_3)_2{\cdot}xH_2O$ Aldrich, 99%) upon addition of an ammoniac solution (28%). The precipitate formed was maintained in the solution under stirring for 1 h and separated by centrifugation. It was washed several times with de-ionized water to eliminate nitrates and dried over night at 110 °C before grinding and calcination at 500 °C for 2 h. Monoclinic zirconia (*m*-$ZrO_2$) has been obtained from Saint-Gobain Norpro (reference: XZ16075).

A sample of the $Zr_{x-2}Nb_2O_{2x+1}$ solid solution with $x = 9$ referred as $Zr_7Nb_2O_{19}$, has been prepared using a sol–gel process [24]. Briefly, 10 g of Pluronic P-123 surfactant (BASF) was added under stirring to 120 mL of anhydrous ethanol (Fluka). About 87.5 mmol of $ZrCl_4$ (Aldrich, 99.5%) and 25 mmol of $NbCl_5$ (Aldrich, 99%) were added to the solution (Zr/Nb molar ratio equal to 3.5). The mixture was stirred for 30 min and maintained at 60 °C for one week. The brown solid obtained was calcined at 350 °C for 20 h to decompose the surfactant and then at 740 °C for 10 h to crystallize the phase and eliminate the possible traces of chlorine.

Two zirconia supported $Nb_2O_5$ catalysts have been prepared by impregnation. The support corresponds to a mixture of tetragonal and monoclinic phases with a specific surface area of 95 $m^2\ g^{-1}$. It was obtained calcining zirconium hydroxide at 600 °C for 2 h. Ten gram of the support was added to a 50 mL aqueous solution containing 2.5 and 5.9 mmol of ammonium oxalato-niobate, respectively, (corresponding to a Nb surface density of 3.3 and 6.6 atom $nm^{-2}$ or 30% and 60% of a theoretical $Nb_2O_5$ monolayer). The solution was aged for 1h30 at room temperature under stirring, evaporated under vacuum, and calcined at 600 °C for 2 h (heating rate 5 °C $min^{-1}$). The solids will be designated as $NbO_x$-0.3/$ZrO_2$ and $NbO_x$-0.6/$ZrO_2$.

#### 2.1.3. Reference catalysts

Reference catalysts have been used to compare the catalytic properties of the prepared catalysts. These reference catalysts correspond to a commercial tungstated zirconia from Daiichi Kigenso Kagaku Kogyo (reference Z-1104) and a commercial ZSM5 from Zeochem (reference Zeocat PZ2/50H). The references are respectively denoted ZrWO-DKK and HZSM-5.

### 2.2. Catalysts characterization

Metal contents of the mixed oxides were determined by atomic absorption (ICP) and their specific surface areas were determined using the BET method with nitrogen adsorption. Powder X-ray diffraction (XRD) patterns were obtained using a BRUKER D5005 diffractometer with Cu Kα radiation ($\lambda = 0.154184$ nm). They were recorded with 0.02 ($2\theta$) steps over 10–80 angular range with 10 s counting time per step. The unit cell of the zirconia phase was refined using Bruker Topas P program.

Raman spectra were recorded using a LabRam HR spectrometer (Jobin Yvon-Horiba). The exciting line at 514.53 nm of an Ar–Kr 2018 RM laser (Spectra Physics) was focused on several points of the samples with a long working X50 objective. The laser power on samples was limited to 1 mW. Several points were analyzed to control the samples homogeneity at the micron scale.

Surface analyses by X-ray photoelectron spectroscopy (XPS) were performed in a KRATOS Axis Ultra DLD equipped with a magnetic immersion lens, a hemispherical analyzer, and a delay line detector. Experiments were carried out using a monochromated Al Kα X-ray source with a pressure below $5 \times 10^{-8}$ Pa in the analysis chamber. XPS spectra of $Zr3d_{5/2}$, $Nb3d_{5/2}$, $O_{1s}$, and $C_{1s}$ levels were measured at 90° (normal angle with respect to the plane of the surface). A charge neutralizer was used to control charges effects on samples.

Samples were characterized by solid-state $^{13}C$ CPMAS NMR (100.62 MHz, pulse time 3.5 μs, contact time 3 ms, 10 kHz spinning rate) using a Bruker DSX-400 spectrometer and a 4 mm CPMAS probe to obtain some information on the coke formed at the surface of the catalysts after catalytic testing.

TPD of ammonia was performed on an apparatus Autochem 2910 from micromeritics, with 100 mg of catalysts. The samples were pre-treated 30 min at 300 °C under helium (30 mL $min^{-1}$) and the successively treated in a flux of 5% of ammonia in helium (30 mL $min^{-1}$) for 15 min at room temperature and in helium for 1 h at 100 °C. The temperature of the calorimeter furnace was then programmed with a heating rate of 10 °C $min^{-1}$ at 30 mL $min^{-1}$ helium flow rate. The concentration of ammonia desorbing from the sample was continuously monitored by gas chromatography. The output was then plotted against temperature to get the TPD profile.

### 2.3. Catalysts testing

The prepared solids were tested for dehydration of glycerol at 300 °C under atmospheric pressure using a glass plug-flow micro-reactor. The catalyst volume (4.5 mL) was chosen to obtain complete or near complete glycerol conversion with reference catalysts. Prior to the reaction, the samples were pre-heated at 300 °C for 15 min in flowing $N_2$ (75 mL $min^{-1}$). A 20 wt% aqueous glycerol solution was vaporized with an inert gas flow to the reactor using a Bronkhorst controlled evaporator mixer system. The aqueous glycerol solution was fed at a rate of 3.8 g $h^{-1}$, and the inert gas flow (He/Ne: 90/1) was 75 mL $min^{-1}$ giving a molar relative composition glycerol/water/inert gas of 2.3/46.3/51.4 (GHSV = 1930 $h^{-1}$). CO and $CO_2$ were analyzed online, using a gas chromatograph equipped with a TCD detector and using a Carboxen 1000 column, Ne was used as internal standard. Organic substrates were condensed at low temperature during the reaction and analyzed off line using gas chromatographs equipped with FID detectors and a Nukol column or a ZBwax plus column.

## 3. Results

### 3.1. Study of ZrNbO catalysts

Table 1 provides an overview of the detailed catalytic properties obtained with the ZrNbO catalyst at 300 °C, under standard reaction conditions. These data were obtained after 48 h on stream. The catalysts needed between 10 and 20 h to reach their optimal selectivity, which then remained constant. During this induction period, very strong and thus unselective acid sites should be neutralized by coking. The best selectivity at or near to total conversion, equal to 72%, was obtained with the ZrNbO-12 catalysts. This is slightly lower than the best figures found in the literature, which lie above 80%. However, the catalysts appeared to be very stable on stream, as shown in Fig. 1. For comparison, the evolution of the conversion on reference phases described in the literature (HZSM-5 and ZrWO-DKK), tested under the same conditions, is shown in the same figure. It should be noted that the catalytic performances obtained with the latter phases were similar to those reported in the literature, which tends to confirm the correctness of our data acquisition system. It can be seen in Fig. 1 that the increase in Nb content has a positive effect on the stability of the catalysts. However, when the time on stream was increased, all of the catalysts lost their activity, whereas their selectivity to acrolein remained constant, with no significant changes observed in their by-product distribution.

The ZrNbO catalysts were characterized using X-ray diffraction and Raman spectroscopy. The X-ray diffraction patterns of the ZrNbO samples reveal two phases, corresponding to m and *t*-$ZrO_2$ (Fig. 2). The relative *m*-$ZrO_2$ content increased when the Nb content decreased. This result is in agreement with previous studies showing that niobium helps in the stabilization of the tetragonal form [24,25]. The cell parameters of the *m* and *t*-$ZrO_2$ phases have been calculated for the different compounds (Table 2). They are comparable for the three catalysts, and lower than those of the initially prepared phases without Nb. It can be noticed that the tetragonality of the *t*-$ZrO_2$ phase (the c/a ratio) increased slightly with the Nb content. Similar behavior was already observed with increasing substitution of *t*-$ZrO_2$ by under-sized tetravalent cations [26].

Raman spectroscopy was also used to characterize the ZrNbO catalysts. The spectra recorded at room temperature and at 600 °C are shown in Figs. 3 and 4, respectively. The room temperature spectra were similar and confirmed the presence of both tetragonal and monoclinic zirconia. The Raman bands at 278 and 649 $cm^{-1}$ involve O–Zr–O bending and Zr–O stretching force constants of long Zr–O bonds and O–Zr–O bending force constants

**Table 1**
Catalytic performances of the ZrNbO catalysts. Reaction temperature 300 °C, glycerol aqueous solution (20 wt%) flow rate 3.8 g $h^{-1}$, inert gas flow rate 75 mL $min^{-1}$.

| Catalyst | ZrNbO-12 | ZrNbO-19 | ZrNbO-31 |
|---|---|---|---|
| Specific surface area ($m^2$ $g^{-1}$) | 55 | 53 | 74 |
| Mass of catalyst (g) | 7.5 | 7.5 | 7.5 |
| Reaction time (h) | 48 | 48 | 48 |
| Glycerol conversion (%) | 99 | 100 | 100 |
| Selectivity (%) to | | | |
| Acrolein | 72 | 59 | 51 |
| Acetaldehyde | 3.8 | 5.8 | 7.2 |
| Propanal | 2.1 | 3.3 | 3.9 |
| Acetone | 1.1 | 1.0 | 2.8 |
| 2,3-Butanedione | 0.7 | 0.8 | 0.8 |
| Allylic alcohol | 1.1 | 1.9 | 3.5 |
| Hydroxyacetone | 11.3 | 13.0 | 24.0 |
| Phenol | 0.9 | 0.9 | 0.5 |
| CO | 1.5 | 2.2 | 2.1 |
| $CO_2$ | – | – | – |
| Carbon balance (%) | 95 | 89 | 97 |

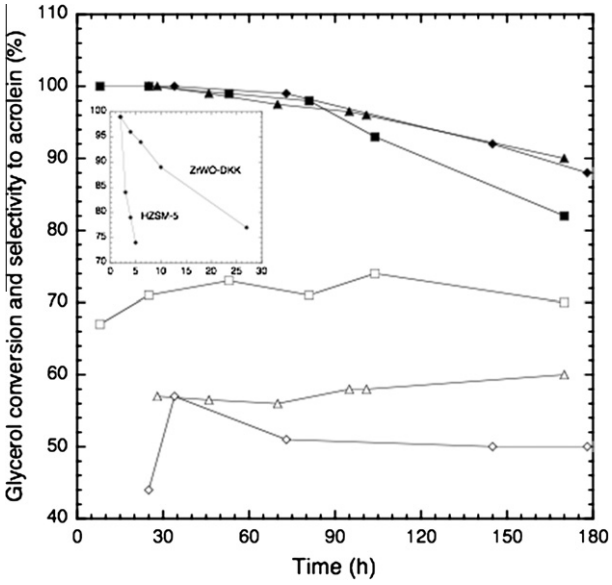


**Fig. 1.** Evolution of glycerol conversion and selectivity to acrolein as a function of time on stream at 300 °C for the ZrNbO-12 catalyst and for HZSM-5 and ZrWO-DKK references. Flow rate of the 20% in weight glycerol solution: 3.8 g $h^{-1}$, flow rate of inert gas: 75 mL $min^{-1}$, volume of catalyst: 4.5 mL.

of short Zr–O bonds, respectively [27], appeared with a shift of 9 $cm^{-1}$ toward a higher frequency when compared to pure zirconia, thus indicating an increase in the zirconium–oxygen bond strength. This result can be explained by the formation of a solid solution of Nb into $ZrO_2$. In addition to the bands attributed to *t*-$ZrO_2$ (150, 278, 316, 457, and 649 $cm^{-1}$) and to *m*-$ZrO_2$ (179, 190, 223, 332, 378, 474, 558, and 558 $cm^{-1}$), the room temperature spectra revealed a large band centered at 774 $cm^{-1}$, which has previously been attributed to stretching frequencies of niobium–oxygen (Nb–O) bonds in a nearly perfect $NbO_4$ environment [28]. A similar band was observed in the $ZrO_2$–$Y_2O_3$–$Nb_2O_5$

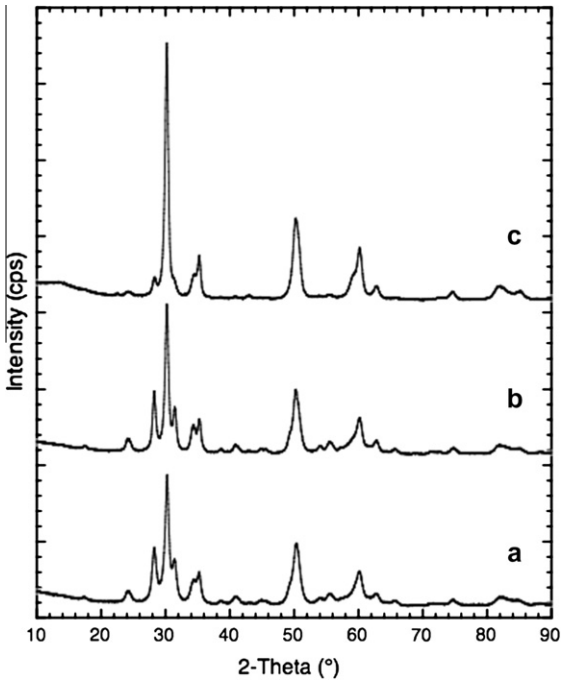


**Fig. 2.** X-ray diffraction patterns of the catalysts (a) ZrNbO-31, (b) ZrNbO-19 and ZrNbO-12 (c) catalysts.

**Table 2**
Cell parameters of the m- and t-$ZrO_2$ of the ZrNbO and $NbO_x/ZrO_2$ catalysts calculated from X-ray diffraction data.

| Catalyst | *t*-$ZrO_2$ cell parameters | | | *m*-$ZrO_2$ cell parameters | | | | |
|---|---|---|---|---|---|---|---|---|
| | *a* (nm) | *c* (nm) | *V* ($nm^3$) | *a* (nm) | *b* (nm) | *c* (nm) | *β* (°) | *V* ($nm^3$) |
| $NbO_x$-0.3/$ZrO_2$ | 0.3631(3) | 0.5092(5) | 0.0671 | 0.5155(9) | 0.5247(7) | 0.5266(4) | 81.301(2) | 0.1407 |
| $NbO_x$-0.6/$ZrO_2$ | 0.3634(5) | 0.5094(5) | 0.0672 | 0.5158(9) | 0.5250(7) | 0.5265(8) | 81.347(2) | 0.1408 |
| ZrNbO-31 | 0.3594(1) | 0.5171(3) | 0.0667 | 0.5145(3) | 0.5233(4) | 0.5257(3) | 81.168(3) | 0.1398 |
| ZrNbO-19 | 0.3598(1) | 0.5177(3) | 0.0669 | 0.5135(2) | 0.5236(2) | 0.5257(2) | 81.129(9) | 0.1384 |
| ZrNbO-12 | 0.3594(1) | 0.5180(2) | 0.0669 | 0.5140(3) | 0.5236(4) | 0.5246(4) | 81.129(3) | 0.1383 |

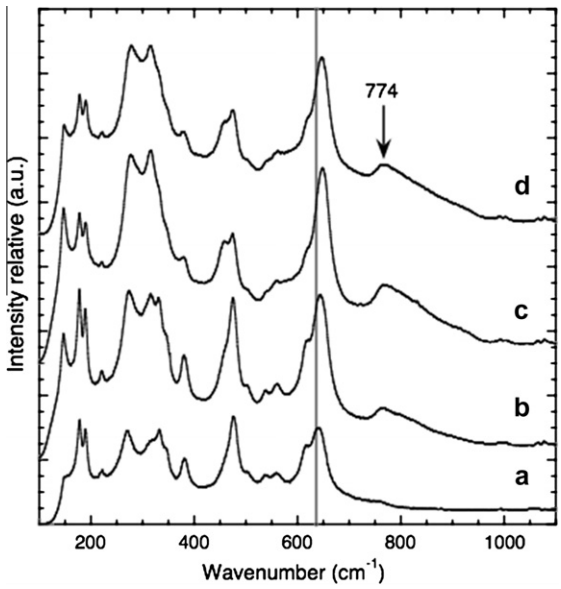


**Fig. 3.** Raman spectra of (a) zirconia (b) ZrNbO-31, (c) ZrNbO-19, and (d) ZrNbO-12 at room temperature in ambient air.

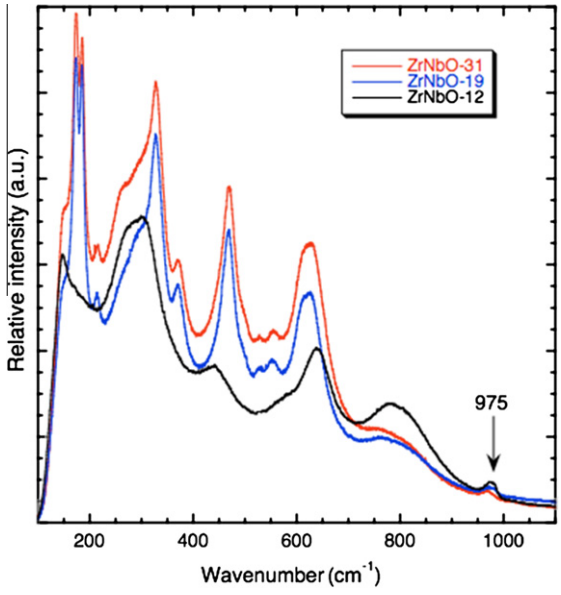


**Fig. 4.** Raman spectra of the catalyst at 600 °C under dry air (a) ZrNbO-31, (b) ZrNbO-19, and (c) ZrNbO-12.

system and was attributed to $NbO_4$ tetrahedra in $ZrO_2$ [29]. In tetragonal zirconia, Zr cations have eightfold coordination to oxygen with 4 O at 0.207 nm and 4 O at 0.245 nm. The 4 first oxygen anions form regular tetrahedra, which would fit with the presence

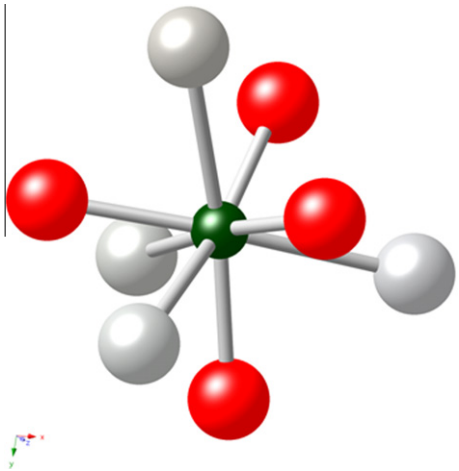

**Fig. 5.** Schematic representation of Zr environment in *t*-$ZrO_2$ with 4 oxygen at 0.2453 nm and 4 oxygen at 0.2072 nm forming a regular tetrahedron (all O–Zr–O equal to 103.215).

of the $NbO_4$ tetrahedra in the case of Nb substitution to Zr (Fig. 5). The stretching frequencies of the niobium–oxygen (Nb–O) bonds of the supported niobium species are normally observed in the range between 850 and 930 $cm^{-1}$ in ambient air [30]. However, the presence of hydration water leads to van der Waals interactions, which weaken and enlarge the corresponding bands, such that it is preferable to dehydrate the compound, in order to highlight these bands. The Raman spectra were thus recorded under dry air conditions at 600 °C (Fig. 4). All of these are characterized by a band at 977 $cm^{-1}$, which is intermediate between the frequencies observed for niobium oxide supported on zirconia with a low content (1%, 958 $cm^{-1}$), and that with a high content (5%, 988 $cm^{-1}$), which almost corresponds to a monolayer [31]. The catalysts should thus contain niobium oxide supported on zirconia as polymers. The nuclearity of these polymers should vary strongly, as evidenced by the high width of the bands. Finally, it should be emphasized that during Raman spectroscopy measurements, several areas of each catalyst were analyzed under the microscope. Point-to-point comparison of the spectra has shown good homogeneity of the catalysts and confirmed the absence of other phases such as bulk niobium oxide. In the case of the ZrNbO-12 sample only, very few analyses were able to reveal the presence of the $Zr_7Nb_2O_{19}$ phase, with its characteristic band at 418 $cm^{-1}$. As the presence of this phase was not detected by X-ray diffraction, it is known to have been present in only very small quantities.

### 3.2. Study of pure bulk and supported phases

In order to understand the origin of the catalytic properties of the catalysts, the phases detected by X-ray diffraction or Raman spectroscopy were synthesized in their pure form a and tested as

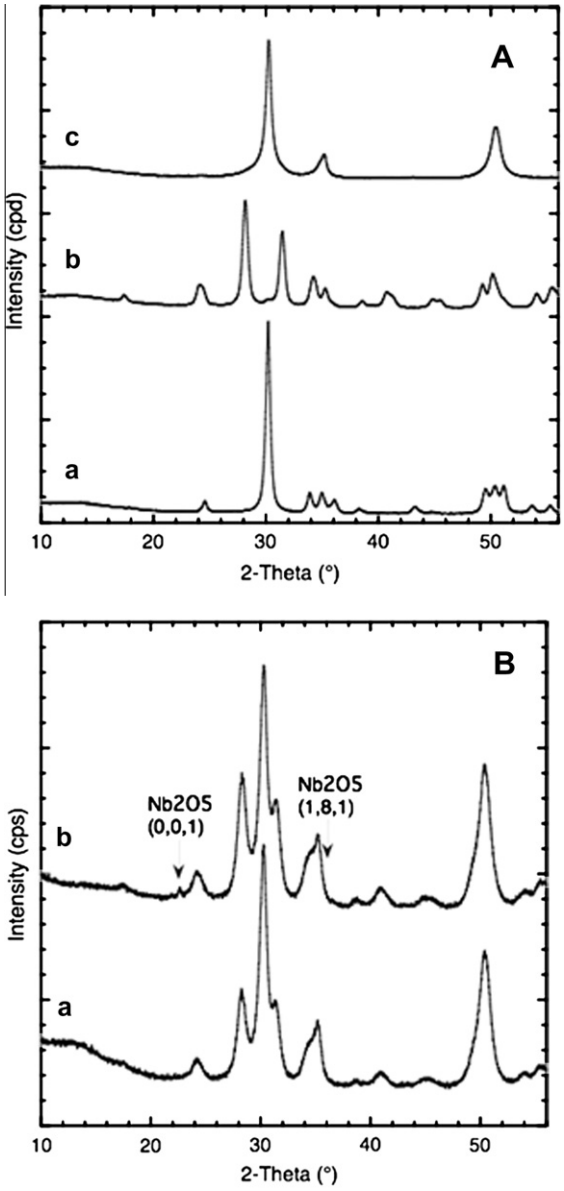


**Fig. 6.** X-ray diffraction pattern of the pure phases A: (a) $Zr_7Nb_2O_{17}$, (b) *m*-$ZrO_2$, (c) *t*-$ZrO_2$ and of the supported $NbO_x/ZrO_2$ catalysts B: (a), $NbO_x$-0.3/$ZrO_2$, (b) $NbO_x$-0.6/$ZrO_2$.

catalysts, as well as catalysts corresponding to niobium oxide supported on zirconia. The X-ray diffraction pattern of $Zr_7Nb_2O_{19}$, the two $ZrO_2$ phases (*m* and *t*), and two Nb supported catalysts with different niobium contents are presented in Fig. 6. The pattern of the mixed zirconium and niobium compound corresponds well to the pure phase (ICSD: 012-2312). The patterns of the Nb supported catalysts ($NbO_x$-0.3/$ZrO_2$ and $NbO_x$-0.6/$ZrO_2$) reveal the presence of both monoclinic and tetragonal zirconia. They are similar, apart from the fact that very small peaks corresponding to $Nb_2O_5$ (ICSD: 027-1003) can be seen in the $NbO_x$-0.6/$ZrO_2$ pattern. The homogeneous spreading of niobium at the surface of already crystallized zirconia is difficult, and niobium oxide is formed before a quantity of niobium equivalent to a monolayer can be deposited.

The pure phases and supported catalysts were tested as catalysts (Table 3). The pure zirconia phases appeared to be active, but not selective to acrolein, and hydroxyacetone was the major product formed on these phases. The $Zr_7Nb_2O_{19}$ phase was both active and selective, although less than the ZrNbO catalysts, and markedly less stable. The catalytic properties of the $NbO_x/ZrO_2$ catalysts with different Nb contents (−0.3 and −0.6) appeared to be similar. The solids are more active, selective, and stable than the pure $ZrO_2$ phases. However, their performance did not attain that of the ZrNbO catalysts. The similarities in catalytic performance of the two $NbO_x/ZrO_2$ catalysts can be explained by the fact that, because of the formation of bulk $Nb_2O_5$ in the case of the catalysts with the richer Nb content, the two catalysts most likely have similar niobium dispersion characteristics at the surface of zirconia. Since the bulk niobium oxide phase obtained after heat treatment at 600 °C is poorly active in the reaction [21], it is understandable that the catalytic data are the same for the two catalysts. It should be noted that the literature reports homogeneous dispersion of niobium at the surface of zirconia, with a thickness greater than 0.6 monolayer [32]. However, most of the reported data were obtained on a nearly pure monoclinic phase, which is not the case of the solids containing large quantities of the tetragonal phase described here.

### 3.3. Surface characterization of the catalysts

The results obtained on the pure phases and the $NbO_x/ZrO_2$ catalysts lead to the conclusion that the catalytic properties of the ZrNbO catalysts are related to the surface niobium polymer species formed by the new preparation method. It was thus important to achieve improved characterization of the surface of the catalysts. This was done using XPS spectroscopy and ammonia TPD.

The results obtained with XPS spectroscopy are presented in Table 4. They show that the surface of the ZrNbO was richer in Nb than the bulk material, which is in agreement with Raman spectroscopy showing the presence of surface polymeric niobium oxide species. Furthermore, analysis of the $C_{1s}$ signal revealed the presence of a carbonate species (288.8 ± 0.001 eV) at the surface of the catalysts, the quantity of which decreased when the Nb content increased. The carbonate species results from the adsorption of atmospheric $CO_2$ by the strongly basic oxygen ions (Lewis type) of the uncovered zirconium oxide. It should be pointed out that the $Zr_7Nb_2O_{19}$ mixed oxide has a relatively high surface content of strong basic sites.

Fig. 7 and Table 5 show the ammonia TPD results on different samples. All of the thermograms have two broad maxima: the first of these is found at approximately 170 °C, and the second occurs in

**Table 3**
Catalytic performances of the single phases and $NbO_x$ supported zirconia-based catalysts. Reaction temperature 300 °C, glycerol aqueous solution (20 wt%) flow rate 3.8 g $h^{-1}$, inert gas flow rate 75 mL $min^{-1}$.

| Catalyst | SA ($m^2$ $g^{-1}$) | *m* (g) | TOS (h) | Conv. (%) | $S_{AC}$ (%) | $S_{HA}$ (%) | CB (%) |
|---|---|---|---|---|---|---|---|
| $Zr_7Nb_2O_{19}$ | 41 | 7.5 | 8 | 88 | 60 | 7.6 | 88 |
| $NbO_x$-0.3/$ZrO_2$ | 88 | 8.9 | 8 | 99 | 35 | 5.7 | 74 |
| $NbO_x$-0.6/$ZrO_2$ | 84 | 8.9 | 7 | 100 | 35 | 2.6 | 66 |
| *m*-$ZrO_2$ | 53 | 7.5 | 8 | 97 | 7 | 36.0 | 65 |
| *t*-$ZrO_2$ | 98 | 3.8 | 10 | 73 | 21 | 26.0 | 82 |

SA = specific surface area, *m* = mass of catalyst, TOS = time on Stream, Conv = conversion of glycerol, $S_{AC}$ = selectivity to acrolein, $S_{HA}$ = selectivity to hydroxyacetone, CB = carbon balance.

**Table 4**
XPS analyses of different studied catalysts. The surface Nb/Zr ratio is compared with the bulk ratio calculated from results of chemical analyses. B.E.: binding energy.

| Catalyst | Nb/Zr | | B.E. $C_{CO3}$ (eV) | $CO_3$/Zr |
|---|---|---|---|---|
| | Surface | Bulk | | |
| $(m + t)$ $ZrO_2$ | 0.00 | 0.00 | 288.6 | 0.13 |
| NbZrO-31 | 0.15 | 0.03 | 288.7 | 0.10 |
| NbZrO-12 | 0.73 | 0.09 | 288.9 | 0.06 |
| $NbO_x$-0.3/$ZrO_2$ | 0.10 | 0.03 | 288.7 | 0.06 |
| $Zr_7Nb_2O_{19}$ | 0.41 | 0.28 | 288.9 | 0.07 |

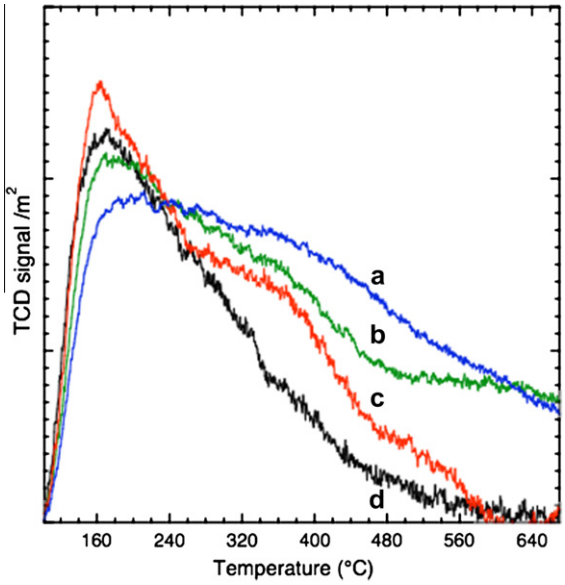


**Fig. 7.** $NH_3$-TPD thermograms of ammonia on different solids: (a) $(m + t)ZrO_2$, (b) $NbO_x$-0.3/$ZrO_2$, (c) ZrNbO-12, (d) $Zr_7Nb_2O_{19}$.

the range between 350 and 400 °C. No shift in the peaks' maxima was observed, from one sample to the other, although it is difficult to define the position of the second peak as a consequence of its broad profile. Compared with the Nb containing solids, $ZrO_2$ exhibited a more intense second peak, which can be attributed to stronger acid sites. The density of strong acid sites is lower on the $NbO_x$/$ZrO_2$ solid and decreased even further on the ZrNbO-12 catalyst presenting a higher Nb surface content. The $Zr_7Nb_2O_{19}$ has a smaller number of weak and strong acid sites.

### 3.4. Study of several reaction parameters and regenerability

The influences of the reaction temperature and the flow rate of the diluting gas on the catalytic properties of the catalysts were studied.

The catalytic properties of the ZrNbO-12 catalyst obtained at different temperatures are presented in Table 6. This catalyst was first tested at 300 °C for 24 h. After that time, the optimal

**Table 5**
Results of $NH_3$ TPD on different catalysts.

| Catalyst | Volume of $NH_3$ adsorbed (mL $g^{-1}$) | First peak temperature (°C) | Total acid site concentration (mmol $m^{-2}$) |
|---|---|---|---|
| ZrNbO-12 | 4.8 | 161 | 3.5 |
| $ZR_7Nb_2O_{19}$ | 2.9 | 170 | 3.0 |
| $NbO_x$-0.3/$ZrO_2$ | 9.0 | 168 | 4.8 |
| $(m + t)$ $ZrO_2$ | 11.4 | 211 | 4.5 |

**Table 6**
Catalytic performances of the ZrNbO catalysts at different reaction temperature, glycerol aqueous solution (20 wt%) flow rate 3.8 g $h^{-1}$, inert gas flow rate 75 mL $min^{-1}$, catalyst volume 4.5 mL (7.5 g).

| | | | |
|---|---|---|---|
| Reaction temperature (°C) | 280 | 290 | 300 |
| Glycerol conversion (%) | 64 | 93 | 100 |
| Reaction time (h) | 24 | 28 | 32 |
| Selectivity (%) to | | | |
| Acrolein | 71.0 | 71.0 | 70.0 |
| Acetaldehyde | 1.5 | 2.4 | 4.5 |
| Propanal | 1.0 | 1.4 | 2.6 |
| Acetone | 0.2 | 0.3 | 0.8 |
| 2,3-Butanedione | 0.0 | 0.3 | 0.8 |
| Allylic alcohol | 1.1 | 1.3 | 1.3 |
| Hydroxyacetone | 16.6 | 16.3 | 11.8 |
| Phenol | 0.1 | 0.3 | 1.1 |
| CO | 1.5 | 2.2 | 2.1 |
| $CO_2$ | – | – | – |
| Carbon balance (%) | 96 | 97 | 100 |

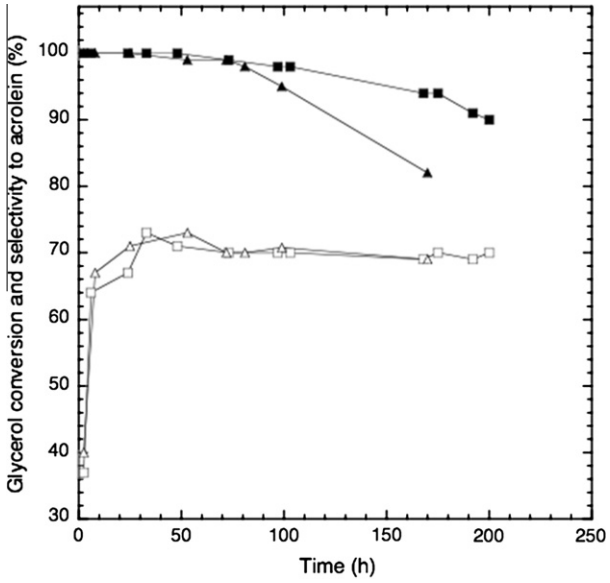


**Fig. 8.** Evolution of glycerol conversion and selectivity to acrolein as a function of time on stream at 300 °C for the ZrNbO-12 catalyst with inert gas flow rates of 75 mL $min^{-1}$ (black and white triangles) and 200 mL $min^{-1}$ (black and white squares). Flow rate of the 20% in weight glycerol solution: 3.8 g $h^{-1}$, flow rate of inert gas: 75 mL $min^{-1}$, and volume of catalyst: 4.5 mL.

selectivity to acrolein was obtained, and the reaction temperature was decreased successively to 290 °C, and then to 280 °C, for testing. When the temperature decreased the activity of the catalyst decreased, but the selectivity to acrolein did not change. In parallel, the selectivity to hydroxyacetone increased, and that to acetaldehyde, 2,3-butanediol and phenol decreased. This can be explained by the fact that hydroxyacetone is decomposed to a lesser extent and that the latter compounds are the products of this decomposition. Because several of these products are suspected to be coke formation precursors, it is probable that a lower reaction temperature led to an improved temporal stability of the catalysts.

The effect of flow rate of the diluting gas was studied by testing the same catalyst under the same conditions, with the exception of the nitrogen flow, which was increased from 75 to 200 mL $min^{-1}$. The glycerol contact time was thus decreased from 1.9 to 1.0 s. As seen in Fig. 8, the increase in nitrogen flow rate had no influence on the selectivity to acrolein, but slowed the deactivation rate. With a 200 mL.$min^{-1}$ nitrogen flow rate, the glycerol conversion still remained at approximately 90% after 200 h, with selectivity to acrolein of 71%. The increase in nitrogen flow rate delayed the

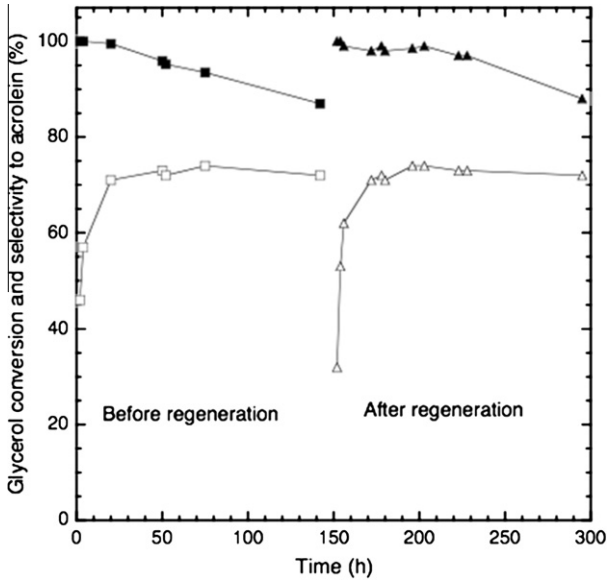


**Fig. 9.** Evolution of the glycerol conversion and acrolein selectivity as a function of time at 300 °C for 150 h before and after an in situ regeneration at 450 °C in air for 1 h. Flow rate of the 20% in weight glycerol solution: 3.8 g $h^{-1}$, flow rate of inert gas: 75 mL $min^{-1}$, and volume of catalyst: 4.5 mL.

formation of coke by reducing the residence time of coke precursors in the reactor.

Although the ZrNbO catalysts appeared to be relatively stable, the introduction of a regeneration step into the process using these catalysts needs to be envisaged. It was thus important to determine whether regeneration based on a simple heat treatment in an oxidative atmosphere, designed to burn the coke formed at the surface of the catalysts, could be efficient. After 150 h on stream, the reaction flow was switched to an air-flow (75 mL $min^{-1}$), the temperature was increased to 450 °C and maintained at this temperature for 1 h. The catalyst was then cooled down to the catalytic reaction temperature, and the initial catalytic reaction flow re-introduced. The variations in glycerol conversion and selectivity to acrolein are plotted as a function of time, before and after this treatment (Fig. 9). It can be seen that the catalytic properties were recovered following the heat treatment. The same initial period for selectivity optimization and the same deactivation as a function of time on stream, with the same deactivation rate, were observed. The catalysts are thus fully regenerated by the heat treatment in air.

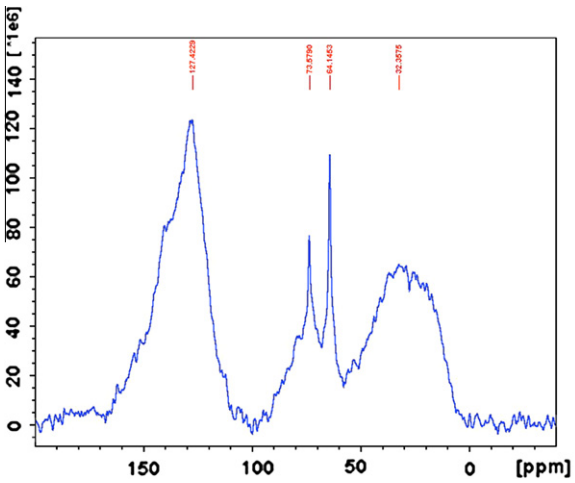


**Fig. 10.** $^{13}C$ CP-MAS n.m.r. spectrum of coke on spent catalyst.

The carbon deposited at the surface of the ZrNbO catalyst was characterized by $^{13}C$ NMR testing. The spectrum obtained with a ZrNbO catalyst after catalytic testing was characterized by two large bands around 127 and 32 ppm corresponding to aromatic and aliphatic carbons, respectively (Fig. 10) [33]. The two narrow peaks at 64 and 74 ppm were attributed to adsorbed glycerol, or products derived from glycerol such as polyglycerols or acetalization products of glycerol, adsorbed onto the surface of the catalyst. All of these detected species can be expected to contribute to the deactivation of the catalysts. It is believed that coke formation occurs on strong catalyst acid sites, and that polyglycerols or acetalization products of glycerol are formed and remain adsorbed on basic sites [34,35]. Both types of site are certainly involved in the deactivation of the catalysts.

## 4. Discussion

The results obtained show that the ZrNbO catalysts prepared according to the protocol described in the experimental section are efficient for the dehydration of glycerol to acrolein. With a total conversion of only 72%, they do not have the best selectivity to acrolein, when compared to other catalysts such as heteropolyacid-based catalysts, whose selectivity exceeds 80% [36]. It should be emphasized that it is not straightforward to compare ZrNbO catalysts with other catalysts, tested under the same conditions, since the former have not reached their optimal selectivity at the time when the latter have already undergone very strong deactivation. This feature is related to the incomparable stability of the ZrNbO catalysts, which maintain a glycerol conversion greater than 90% for more than 200 h (Fig. 8), whereas other catalysts are almost completely deactivated after the same time on stream. It should be mentioned that the catalytic sites in the catalysts might not be all working at the beginning of the testing since it is difficult to adjust the mass of catalyst to have exactly 100% glycerol conversion. It is thus possible that the stability may be over-estimated by some hours, but this should be very limited compare with the total time on stream.

Characterization of the ZrNbO catalysts has shown that the active species correspond to polymeric $NbO_x$ species at the surface of the zirconia support. Such supported species have already been shown to generate Brønsted acid sites, which are active and selective for the dehydration reaction [32,37].

Ammonia TPD experiments clearly show that these acid sites are, in general, relatively weak. If the catalytic properties of the ZrNbO catalysts are related to the polymeric species distributed over the surface of zirconia, the $NbO_x/ZrO_2$ catalyst should exhibit similar catalytic properties. However, the latter type of catalyst is neither as selective nor as stable. The characterization clearly showed that for $NbO_x/ZrO_2$ catalysts, contrary to the case of ZrNbO catalysts, no solid solution of Nb was formed into $ZrO_2$. The formation of this solid solution thus appeared to be a key element in obtaining highly efficient catalysts.

The formation of the solid solution of Nb into $ZrO_2$ is related to the preparation protocol used for the synthesis of the catalysts, which facilitated the formation of such a solid solution. The preparation was conducted in water at pH < 0.5. At this pH, the niobium species present should correspond to the anionic species $[NbO(C_2O_4)(OH)_2(H_2O)]^-$ or $[NbO(OH)_4(H_2O)]^-$ [38], which could efficiently exchange with $[OH]^-$ groups of the zirconium hydroxide $Zr(OH)_4$ precursor. Such an exchange is not possible, or remains very limited, for catalysts prepared by the impregnation of $ZrO_2$ supports, with a prior heat treatment at 600 °C, as in the case of the $NbO_x/ZrO_2$ catalysts.

The dissolution of Nb is accompanied by a decrease in the lattice parameters of the zirconium oxide phase. This may be related to the fact that the cationic size of $Nb^{5+}$ (0.070 nm) is smaller than the cationic size of the host $Zr^{4+}$ (0.084 nm) ion. These results are in agreement with those given in the literature [39], which also report that at thermodynamic equilibrium the solid solution of Nb in $ZrO_2$ reached a concentration of at least 5% (Zr/Nb = 9.5). Although the starting solid composition of the catalysts could only allow the formation of such a solid solution, the latter is not completely formed. Because the Nb and Zr homogeneity in the formed precursor is not optimal, and because the heating temperature, i.e., 600 °C, is not sufficiently high, a completely homogeneous solid solution is not formed and part of the niobium remains at the surface of the catalyst in the form of a polymeric species.

The significant formation of the solid solution certainly allows the number of strong acid sites (Lewis type acid sites) present at the surface of the $ZrO_2$ support phase to be decreased, as well as the number of basic sites as evidenced by XPS spectroscopy. These later sites have been shown to be unselective for glycerol dehydration to acrolein [16,40]. They may also be responsible like the strong acid sites, but to a lower extend, for the low stability of the catalysts. With that respect several studies have shown that the coke loadings were higher on most acidic catalysts [20,21,41]. The deactivation of catalysts for glycerol dehydration, through the deposition of carbon on their surface during the catalytic reaction, may also be influenced by several other parameters such as the reaction temperature, the reactant feed, and the porosity of the support. For the ZrNbO catalysts, a pore size of approximately 7 nm and a reaction temperature of 300 °C appeared to be efficient parameters for long-term stability. A more complete study would be needed, to determine whether these are the optimum values for long-term stability. A high diluting gas flow rate, which reduces the residence time of coke precursors in the reactor, has also been shown to decrease the rate of deactivation. For such a case, a compromise between the slower deactivation and the lower productivity needs to be found.

The bulk $Nb_2O_5$ phase and $Nb_2O_5$ supported on silica have both been shown to be active and selective catalysts for the dehydration of glycerol [18,41]. It is thus not surprising that niobium oxide supported on zirconia is an efficient catalyst for this reaction. Zirconia certainly has an effect on the strength of the supported species, or on their stabilization, which leads to better catalytic properties. It is noteworthy that niobium-based oxides have mainly Brønsted acid sites, but also Lewis acid sites at their surface [42]. Although most papers agree that Brønsted acid sites are the most active and selective for the dehydration of glycerol, the precise influence of Lewis acid sites remains unknown. Studies have been undertaken in order to better characterize the acid–base properties of the new catalyst described here and to ascertain the effect of a zirconia support for the niobium species, as well as the role of Lewis acid sites.

It is important to note that a previous study of a $Nb_2O_5$-based catalyst for an acid catalyzed reaction reported that it was particularly resistant to coking [42]. It is thus credible that the high stability of the catalyst is related not only to the neutralization of the Lewis acid and basic sites of the zirconia support, by incorporation of niobium into zirconia, but also to an intrinsic property of the niobium oxide species.

The formation of the solid solution of Nb in $ZrO_2$ has implications in terms of the nature of the zirconia phase formed, since Nb is an effective agent for the stabilization of *t*-$ZrO_2$, when prepared above 600 °C [24]. In this respect, the relative *t*-$ZrO_2$ content increased considerably, in accordance with the Nb content of the catalysts. However, it is rather difficult to ascertain the influence of the $ZrO_2$ structure (monoclinic or tetragonal) on the catalytic performance of the catalysts. In the case of $WO_x/ZrO_2$ catalysts, various discrepancies can be found in the literature. Some authors have reported that the presence of tungsten oxide species on monoclinic zirconium oxide does not activate the catalyst for isomerization reactions, because they exhibit only a weak acidity [43,44], whereas other authors did not note any difference [45]. Presumably, in the study reported here, since the strength of the active acid sites is weak, the nature of the zirconia phase may not be a key factor, unless the non-selective zirconia sites are neutralized.

The compound $Nb_2Zr_6O_{17}$, which is a solid solution composition with a modulated structure of the type $Nb_2Zr_{x-2}O_{2x+1}$, with $7.1 \leqslant x \leqslant 10.3$ [46], is characterized by a relatively high selectivity to acrolein. This may be related to the presence of mainly weak acid sites at its surface, with even fewer strong acid sites than the most selective ZrNbO-12 catalyst. However, conversion on this catalyst is not stabilized as a function of time, when on stream. This may be explained by the presence of a higher content of basic sites, as detected by XPS characterization, which could be responsible for deactivation. Experiments conducted on basic catalysts have shown that these types of catalyst are poorly active and unstable [41].

## 5. Conclusion

This study has demonstrated that ZrNbO mixed oxides are selective catalysts for the dehydration of glycerol to acrolein at 300 °C. These new catalysts appear to be particularly efficient, since they deactivated only very slowly by coking. The efficiency of the catalysts is related to that of the catalytic acid sites contributed by the niobium species, supported on zirconia, but also to the neutralization of the non-selective sites of the support. The method used to prepare the catalysts appears to be determinant in generating both features, since it allows the formation of a solid solution of Nb in $ZrO_2$, evidenced both by X-ray diffraction and Raman spectroscopy, and the spreading of polymeric niobium oxide species at the surface of this solid solution. The results show that the same catalyst could not be reproduced simply by grafting niobium oxide onto the surface of zirconia. The deactivation has been shown to be related to the formation of coke on strong Lewis acid sites and eventually to the adsorption of polyglycerol on basic sites at the surface of the catalysts. Both types of non-selective sites present at the surface of the uncovered zirconia should be annihilated by the dissolution of Nb into zirconia, which explains the high stability of the prepared NbZrO catalysts. Although deactivation is strongly slowed on these catalysts, it still occurs. However, a simple treatment with flowing air at a higher temperature than the reaction temperature was found to be sufficient to completely regenerate the deactivated catalysts back to their original level of activity. This is a positive point for a possibly industrialized process. Finally, it is noteworthy that the catalysts' composition was not fully optimized, such that there is room for further improvement. The reaction conditions could certainly also be optimized.

## Acknowledgments

We gratefully acknowledge ADISSEO for financial support. We thank C. Lorentz and P. Delichere for $^{13}C$ NMR and XPS analyses.

## References

[1] M. Pagliaro, M. Rossi, The future of glycerol: new usages for a versatile raw material, RSC Green Chem. Ser. (2008).
[2] A. Behr, J. Eilting, K. Irawadi, J. Leschinski, F. Lindner, Green Chem. 10 (2008) 13.
[3] B. Katryniok, S. Paul, M. Capron, F. Dumeignil, ChemSusChem 2 (2009) 719.
[4] C.J. Zhou, C.J. Huang, W.G. Zhang, H.S. Zhai, H.-L. Wu, Z.S. Chao, Stud. Surf. Sci. Catal. 165 (2007) 527.

[5] A. Corma, G.W. Huber, L. Sauvanaud, P. O'Connor, J. Catal. 257 (2008) 163.
[6] W. Suprun, M. Lutecki, T. Haber, H. Papp, J. Mol. Catal. A: Chem. 309 (2009) 71.
[7] C.J. Jia, Y. Liu, W. Schmidt, A.H. Lu, F. Schueth, J. Catal. 269 (2010) 71.
[8] M. Okuno, E. Matsunami, T. Takahashi, H. Kasuga, M. Okada, M. Kirishik, WO 2007132926, 2007.
[9] X.Z. Li, CN 101070276, 2007.
[10] E. Tsukuda, S. Sato, R. Takahashi, T. Sodesawa, Catal. Commun. 8 (2007) 1349.
[11] H. Atia, U. Armbruster, A. Martin, J. Catal. 258 (2008) 71.
[12] L. Ning, Y. Ding, W. Chen, L. Gong, R. Lin, Y. Lü, Q. Xin, Chin. J. Catal. 29 (2008) 212.
[13] J.L. Dubois, Y. Magatani, K. Okumura WO 2009127889, 2009 (Arkema).
[14] A. Alhanash, E.F. Kozhevnikova, I.V. Kozhevnikov, Appl. Catal. A: Chem. 378 (2010) 11.
[15] J.L. Dubois, C. Duquenne, W. Hoelderich, J. Kervennal, WO 2006087084, 2006.
[16] A. Ulgen, W. Hoelderich, Catal. Lett. 131 (2009) 122.
[17] W. Hoelderich, A. Uelgen, DE 102008027350, 2009.
[18] N.R. Shiju, D.R. Brown, K. Wilson, G. Rothenberg, Top. Catal. 53 (2010) 1217.
[19] H. Redlingshoefer, C. Weckbecker, K. Huthmacher, A. Doerflein, WO 200809254, 2008.
[20] Q. Liu, Z. Zhang, Y. Du, J. Li, X. Yang, Catal. Lett. 127 (2009) 419.
[21] S.H. Chai, H.-P. Wang, Y. Liang, B.-Q. Xu, Green Chem. 9 (2007) 1130.
[22] F. Wang, J.L. Dubois, W. Ueda, J. Catal. 268 (2009) 260.
[23] M. Kantcheva, H. Budunoglu, O. Samarskaya, Catal. Commun. 9 (2008) 874.
[24] D. Lu, B. Lee, J. Kondo, K. Domen, Micropor. Mesopor. Mater. 203 (2004) 75.
[25] L. Mestres, M.L. Martinez-Sarrion, O. Castano, J. Fernandez-Urban, Z. Anorg. Allg. Chem. 627 (2001) 294.
[26] F. del Monte, W. Larsen, J.D. Mackenzie, J. Am. Ceram. Soc. 83 (2000) 628.
[27] P. Bouvier, H.C. Gupta, G. Lucazeau, J. Phys. Chem. Sol. 62 (2001) 873.
[28] F.D. Hardcastle, I.E. Wachs, Solid State Ionics 45 (1991) 201.
[29] D.Y. Lee, J.W. Yang, D.J. Kim, Ceram. Int. 27 (2001) 291.
[30] J.M. Jehng, I.E. Wachs, J. Mol. Catal. 67 (1991) 369.
[31] L.J. Burcham, J. Datka, I.E. Wachs, J. Phys. Chem. B 103 (1999) 6015.
[32] T. Onfroy, G. Clet, M. Houalla, J. Phys. Chem. B 109 (2005) 4588.
[33] D.A. Netzel, F.P. Miknis, J.M. Mitzel, Tiejun Zhang, P.D. Jacobs, H.W. Haynes Jr., Fuel 15 (12) (1996) 1397.
[34] M.T. Martinez, M.D. Martinez, J. Osacar, J. Fuel Process. Technol. 18 (1988) 51.
[35] J.M. Clacens, Y. Pouilloux, J. Barrault, Appl. Catal. A 227 (2002) 181.
[36] B. Katryniok, S. Paul, M. Capron, C. Lancelot, V. Bellière-Baca, P. Rey, F. Dumeignil, Green Chem. (2010).
[37] T. Onfroy, G. Clet, S.B. Bukallah, T. Visser, M. Houalla, Appl. Catal. A 298 (2006) 80.
[38] E. Asselin, T.M. Ahmed, A. Alfantazi, Corrosion Sci. 49 (2007) 694.
[39] J.C. Ray, A.B. Panda, C.R. Saha, P. Pramanik, J. Am. Ceram. Soc. 86 (2003) 514.
[40] A.K. Kinage, P.P. Upare, P. Kasinathan, Y.K. Wang, J.S. Chang, Catal. Commun. 11 (2010) 620.
[41] S.H. Chai, H.-P. Wang, Y. Liang, B.-Q. Xu, J. Catal. 250 (2007) 342.
[42] Q. Sun, Y. Fu, H. Yang, A. Auroux, J. She, J. Mol. Catal. A 275 (2007) 183.
[43] Y. Huang, B. Zhao, Y. Xie, Appl. Catal. A 172 (1998) 327.
[44] F. Di Gregorio, N. Keller, V. Keller, J. Catal. 256 (2008) 159.
[45] J.C. Yori, J.M. Parera, Catal. Lett. 65 (2000) 205.
[46] K. Fütterer, S. Schmid, J.G. Thompson, R.L. Withers, Acta Crystallogr. B51 (1995) 688.